İSTANBUL UNIVERSITY PRESS

Physics and Astronomy Reports
PAR 2025, 3 (2), 100–107
DOI: 10.26650/PAR.2025.00011

RESEARCH ARTICLE

A Simple Numerical Model for Exploring Electrostatic Principles: A Multipole Simulation

N. Bhandari[1], and A. Mal[1]

[1]Department of Physics, AJC Bose College, University of Calcutta, 1/1B, AJC Bose Rd, Elgin, Kolkata, West Bengal 700017, India

ABSTRACT

The multipole expansion is a foundational yet conceptually challenging topic in electrostatics. To bridge this pedagogical gap, we present a computational model designed to visualize the fundamental behavior of electric fields originating from various multipole configurations. Based on the superposition principle for discrete charges, the model simulates dipoles, tripoles, quadrupoles, and pentapoles, and calculates the resulting electric field magnitude as a function of distance (r). The results confirm the core theoretical prediction: the power-law decay of the field, given by $E \propto 1/r^{n+2}$, becomes progressively steeper for higher-order multipoles. This work serves as an effective pedagogical tool, demonstrating how computational physics can render abstract theories tangible and thereby enhance the intuitive understanding of fundamental physical principles. Besides this also provides a platform for further exploration, enabling users to extend the model to more complex configurations and compare computational results with analytical predictions in a systematic manner.

Keywords: Physics education, computational physics, electrostatics, electric multipoles, numerical simulation, visualisation.

1. INTRODUCTION

Electrostatics, the study of stationary electric charges and the electric fields and potentials they generate, is a central pillar of classical electromagnetism and continues to serve as a conceptual foundation for much of modern physics and engineering. From the microscopic scale of atomic and molecular structures to the macroscopic realm of dielectric materials, capacitive devices, and large-scale charge distributions, electrostatic principles govern a vast array of physical phenomena. The fundamental quantities in electrostatics, the electric field ($\vec{E}$) and the electric potential (V), provide a complete and self-consistent description of the forces exerted by charges and the energy landscape in which other charges move. For isolated and highly symmetric systems, such as point charges or uniformly charged spheres, these quantities can be computed exactly using Coulomb's law and Gauss's law. However, realistic charge configurations encountered in natural and engineered systems rarely possess such symmetries. Instead, they typically involve extended, irregular, or spatially complex arrangements for which direct analytic evaluation of the potential becomes impractical or impossible. To address this general challenge, physicists employ the *multipole expansion*, a powerful mathematical framework that provides a systematic approximation of the electric potential of a localized charge distribution at points sufficiently far from the source region (Griffiths 2017; Koulouridis 2025; Byczuk & Jakubczyk 2023).

The essence of the multipole technique lies in decomposing the potential into a hierarchy of contributions, each associated with increasingly fine structural information about the charge distribution. The simplest of these, the *monopole term*, corresponds to the total charge and completely determines the long-range behavior of systems with nonzero net charge.

The next term, the *dipole contribution*, describes the first-order separation of positive and negative charges, while the *quadrupole*, *octupole*, and higher-order terms account for progressively more intricate geometric features. This hierarchical structure allows the potential $V(r)$ at a distant point to be written as an infinite series whose terms scale with increasing inverse powers of the distance r. When the condition $r \gg d$ (with d representing the characteristic size of the charge region) is satisfied, higher-order contributions diminish rapidly, and the series can be truncated after the first few nonzero terms without significant loss of accuracy (Jackson 1999).

The physical significance of the multipole expansion extends far beyond its utility as a computational shortcut. Each term in the series encodes essential information about how the geometry, symmetry, and overall arrangement of charges influence the asymptotic behavior of the fields they produce. For instance,

Corresponding Author: N. Bhandari **E-mail:** nayan.physics@outlook.com
Submitted: 19.10.2025 • **Revision Requested:** 11.11.2025 • **Last Revision Received:** 13.12.2025 • **Accepted:** 18.12.2025 • **Published Online:** 31.12.2025

the monopole term decays as $1/r$, reflecting the radial spread of influence from a nonzero total charge. In contrast, the dipole potential decays as $1/r^2$, indicating a more rapidly diminishing field for neutral but polarized systems. Similarly, quadrupole and higher-order terms exhibit even steeper falloff, scaling as $1/r^3$, $1/r^4$, and so on. These characteristic power-law behaviors are not mere mathematical curiosities; they govern long-range interactions in molecular physics (e.g., van der Waals forces), determine radiation patterns in antenna theory, and play critical roles in gravitational physics, where similar multipole structures arise from mass distributions.

Understanding how and why these decay rates emerge is essential for interpreting a wide class of physical systems across multiple disciplines. Despite the conceptual elegance and wide applicability of the multipole expansion, it remains a challenging topic for many students and early-stage researchers (Mazibe et al. 2023). The transition from concrete, intuitive calculations involving point charges to the abstract formalism of multipole moments and spherical harmonics often feels abrupt. The high level of mathematical sophistication required, particularly when dealing with general three-dimensional distributions, can obscure the underlying physical intuition (Puntel et al. 2021; Lineweaver & Patel 2024). As a result, learners may understand the symbolic expressions for multipole terms without grasping their geometric meaning or their consequences for the long-range behavior of fields.

In recent years, computational modeling has emerged as a powerful pedagogical and research tool for overcoming these conceptual hurdles (Tartero & Krauth 2024; van Dijk 2023). By enabling the numerical evaluation of potentials and fields for arbitrary charge configurations, computational approaches make it possible to visualize how different geometric arrangements give rise to distinct multipole moments and characteristic spatial decay patterns. Such simulations bridge the gap between abstract mathematics and intuitive physical understanding, providing learners with immediate feedback, dynamic visualization, and an opportunity to explore "what-if" scenarios that would be inaccessible through purely analytical methods (Sullivan et al. 2023; Cross 2025; Chabay & Sherwood 2008; Moreira & Gavião 2020). Moreover, computational tools allow researchers to test theoretical predictions, analyze complex charge configurations, and develop physical insight in contexts where analytic calculations may be intractable.

The utility of the multipole expansion is not limited to electrostatics; it is a fundamental tool in various fields, notably in astrophysics and theoretical physics. For instance, the gravitational fields of mass distributions are also analyzed using a gravitational multipole expansion. In the context of general relativity, the analysis of gravitational waves, such as those emitted by binary black hole mergers, relies critically on a tensorial multipole expansion. Einstein showed that the waves emitted by slowly changing, weakly gravitating systems are predominantly quadrupolar. Recent research continues to use this formalism to study complex phenomena like the memory effects of gravitational waves and to connect near-zone fields to far-zone radiation through Bondi coordinates. The technique is also used in molecular and materials science to characterize the electrostatic properties of molecules and complex liquid crystals. This versatility underscores the multipole expansion's role as a unifying mathematical principle in physics, connecting the behavior of elementary charges to the dynamics of spacetime itself.

1.1. The Contribution of this Study to the Literature

Computational physics is increasingly recognized as a "third pillar" of science, complementing theory and experiment. Recent systematic reviews have shown that computational simulations offer significant pedagogical benefits, as they facilitate the understanding of abstract concepts, stimulate active learning, and improve academic performance in physics. By enabling the numerical evaluation of potentials and fields for arbitrary charge configurations, computational approaches make it possible to visualize how different geometric arrangements give rise to distinct multipole moments and characteristic spatial decay patterns (Krasnova et al. 2025; Harris et al. 2020).

This approach provides immediate feedback and an opportunity to explore 'what-if' scenarios that are often inaccessible through purely analytical methods (Murray & Hickman 2023; Chabay & Sherwood 2008; Moreira & Gavião 2020). The integration of coding and simulation throughout the curriculum helps students build computational literacy—a necessity for modern scientific work—and connects physical principles to realistic, large-scale problems. Moreover, computational tools allow researchers to test theoretical predictions, analyze complex charge configurations, and develop physical insight in contexts where analytic calculations may be intractable.

Motivated by both the theoretical importance of multipole physics and its pedagogical challenges, the present study employs a straightforward but robust computational framework to investigate the distance dependence of electric potentials and fields generated by several canonical charge configurations. This study utilizes a numerical model constructed using Python and NumPy.

The contribution of this study to the literature is providing an accessible, open-source visualization tool that bridges the gap between the abstract mathematical formalism of the multipole expansion and the concrete physical behavior of electric fields. Specifically, the study systematically and quantitatively verifies the core theoretical prediction—the power-law decay of the field, given by $E \propto 1/r^{n+2}$, for higher-order multipoles—using a reproducible numerical model built on the fundamental superposition principle. This work offers an effective pedagogical platform for exploring how symmetry and charge geometry fundamentally govern the long-range structure of electrostatic fields.

2. METHODOLOGY

The investigation into the distance-dependence of multipole fields was conducted through a numerical simulation. This section details the computational environment, the construction of the multipole models, and the physical principles used to calculate the electric potential and field. The complete Python script used for this study is available in Appendix A for full reproducibility.

2.1. Computational Environment

The simulation was developed and executed using the Python programming language (version 3.x) (Van Rossum & Drake 2009). The numerical calculations and array manipulations were performed with the NumPy library, a standard for scientific computing in Python (Harris et al. 2020). Data visualization and the generation of plots were accomplished using the Matplotlib library (Hunter 2007).

2.2. Model Setup and Multipole Configurations

The core of the simulation involves modeling each multipole as a discrete set of point charges placed symmetrically along a single axis (defined as the z-axis). This one-dimensional arrangement simplifies the analysis while preserving the essential physics of the multipole's far-field behavior. The specific charge magnitudes (q_i) and their positions (z_i) for each configuration were defined as follows, based on standard constructions for pure multipoles (Griffiths 2017):

- **Dipole:** A standard electric dipole was constructed from two point charges: $q_1 = +1.0$ at $z_1 = +0.5$ and $q_2 = -1.0$ at $z_2 = -0.5$. This configuration has a net charge of zero but a non-zero dipole moment.
- **Linear Quadrupole:** Labeled as 'Tripole' in the source code, this configuration consists of three charges: $q_1 = +1.0$ at $z_1 = +0.5$, $q_2 = -2.0$ at $z_2 = 0.0$, and $q_3 = +1.0$ at $z_3 = -0.5$. This arrangement has both a net charge and a net dipole moment of zero, representing a pure linear quadrupole.
- **Linear Octupole:** Labeled as 'Quadrupole' in the code, this four-charge system was defined with charges $q = \{+1.0, -3.0, +3.0, -1.0\}$ at positions $z = \{+0.5, +1/6, -1/6, -0.5\}$. This specific arrangement results in zero net charge, dipole moment, and quadrupole moment, making its leading-order contribution that of a linear octupole.
- **Linear Hexadecapole:** Labeled as 'Pentapole', this five-charge configuration was constructed with charges $q = \{+1.0, -4.0, +6.0, -4.0, +1.0\}$ at positions $z = \{+0.5, +0.25, 0.0, -0.25, -0.5\}$.

This is a classic construction for a linear 16-pole, or hexadecapole, where the net charge, dipole, quadrupole, and octupole moments are all zero.

For clarity and focus on the power-law dependencies, all physical constants were normalized. The Coulomb constant, $k = 1/(4\pi\epsilon_0)$, was set to unity, and charges and distances were treated as dimensionless quantities.

2.3. Calculation of Electric Potential and Field

The electric potential and field were calculated at a series of observation points along the positive z-axis. The range of distances, r, was defined from $r = 0.1$ to $r = 20.0$ in 20,000 discrete steps to ensure high resolution, particularly in the far-field region ($r \gg 1$) where the asymptotic behavior is most apparent.

The calculation is fundamentally based on the principle of superposition (Griffiths 2017). The total electric potential $V(r)$ at an observation point r on the z-axis is the scalar sum of the potentials from each individual charge q_i located at position z_i:

$$V(r) = \sum_{i=1}^{N} \frac{kq_i}{|r - z_i|} \tag{1}$$

where N is the number of charges in the configuration. Since the charge configurations are symmetric and the observation points are along the axis of symmetry, the electric field vector $\vec{E}$ has only a z-component. This component, E_z, was computed by taking the negative gradient of the potential, which simplifies in one dimension to the negative derivative with respect to r:

$$E_z(r) = -\frac{dV(r)}{dr} \tag{2}$$

Alternatively, this can be calculated directly using the superposition principle for electric fields:

$$E_z(r) = \sum_{i=1}^{N} \frac{kq_i}{(r - z_i)^2} \cdot \mathrm{sgn}(r - z_i) \tag{3}$$

The magnitude of this field, $|E_z(r)|$, was used for subsequent analysis and plotting.

3. RESULTS

The numerical simulation, as described in the Methodology, was executed for each of the four multipole configurations. The resulting electric potential and electric field magnitudes were plotted against distance on a logarithmic-logarithmic (log-log) scale to analyze their asymptotic behavior.

3.1. Numerical Analysis

The numerical simulation provides quantitative verification of the theoretical power-law decay for electric potential and field magnitudes, which is visually represented by the slopes in the log-log plots of Figures 1 and 2.

3.1.1. Electric Potential Decay

Figure 1 displays the log-log plot of the electric potential magnitude $|V|$ as a function of distance r. In a log-log plot, the power-law decay $V \propto 1/r^{n+1}$ is represented by a straight line with a slope equal to $-(n + 1)$.

Near-Field Region ($r \ll 1$): All curves exhibit sharp peaks or singularities, such as the peak at $r \approx 0.5$ for the Dipole and Linear Quadrupole lines. These peaks correspond to the observation point being extremely close to the location of the discrete point charges, where the Coulombic effects dominate, and the multipole approximation is invalid.

Far-Field Decay ($r > 1$): In the far-field region (specifically, the linearity is visible for $r > 1$), the lines become straight, confirming the power-law relationship. The numerical analysis in the far-field region ($10 \leq r \leq 20$) yields the following simulated exponents for the potential decay ($V \propto r^{-n}$), matching the theoretical prediction of n:

Dipole (2 charges): The simulated potential exponent is approximately $n \approx 2.00$. This corresponds to a decay of $V \propto 1/r^2$.

Linear Quadrupole (Tripole): The simulated potential exponent is approximately $n \approx 3.00$. This corresponds to a faster decay of $V \propto 1/r^3$.

Linear Octupole (Quadrupole): The simulated potential exponent is approximately $n \approx 4.00$. This corresponds to a decay of $V \propto 1/r^4$.

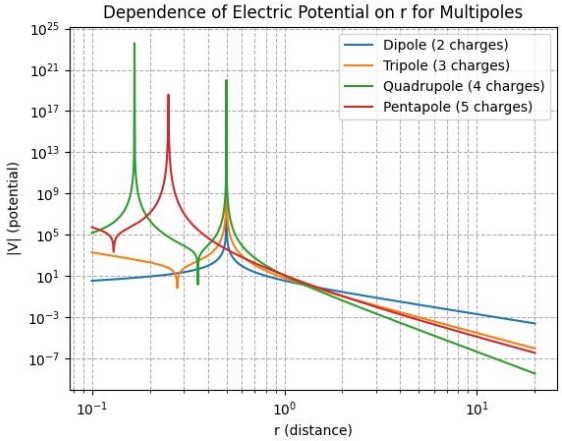

Figure 1. log-log plot of the electric potential magnitude $|V|$ as a function of distance r for the four simulated multipole configurations. The linear behavior in the far-field ($r > 1$) indicates a power-law relationship, with steeper slopes corresponding to higher-order multipoles.

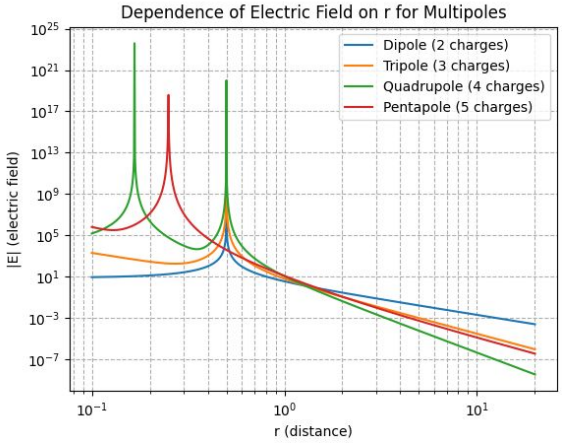

Figure 2. log-log plot of the electric field magnitude $|E|$ as a function of distance r. The slopes in the far-field region are steeper than those for the potential, confirming that the electric field for each multipole decays more rapidly, consistent with theoretical predictions.

Decay Rate: The steepening of the slopes is visually evident. While the slope for the Dipole is approximately -2.00 (decaying as $1/r^2$), it increases in magnitude to -3.00 for the Linear Quadrupole, which aligns with the theoretical prediction of $V \propto 1/r^{n+1}$ where n is the order of the lowest non-zero moment.

3.1.2. Electric Field Decay

Figure 2 shows the log-log plot of the electric field magnitude $|E|$ versus distance r. The electric field for an n-th order multipole is expected to decay as $E \propto 1/r^{n+2}$.

Far-Field Decay: The linear behavior in the far-field region confirms the expected power-law relationship. The decay rates for the electric field are faster (slopes are steeper) than those for the potential, consistent with the field being the spatial derivative of the potential ($E \propto dV/dr$).

The numerical analysis for the field decay ($E \propto r^{-m}$) yields the following simulated exponents, matching the theoretical prediction of $m = n + 2$:

Dipole (2 charges): The simulated field exponent is approximately $m \approx 3.00$. This aligns with the theoretical prediction of $E \propto 1/r^3$.

Linear Quadrupole (Tripole): The simulated field exponent is approximately $m \approx 4.00$. This aligns with the theoretical prediction of $E \propto 1/r^4$.

Linear Octupole (Quadrupole): The simulated field exponent is approximately $m \approx 5.00$. This aligns with the theoretical prediction of $E \propto 1/r^5$.

Decay Rate: The progressive steepening is clear. While the slope magnitude for the Dipole is approximately 3.00 (decaying as $1/r^3$), it increases to 4.00 for the Linear Quadrupole, and further to 5.00 for the Linear Octupole, all of which align with the theoretical prediction of $E \propto 1/r^{n+2}$.

3.1.3. Convergence Region

A significant feature in both Figures 1 and 2 is the common intersection region observed around $r \approx 1$. This point marks the transition between the near-field and far-field regimes, where the magnitudes of the electric field and potential for all configurations converge to comparable values. This indicates the physical boundary where the collective multipole behavior begins to dominate over the localized influence of individual charges.

3.2. Graphical Analysis

The results seen in the plots of Figures 1 and 2 provide a visual confirmation of the theoretical predictions derived from classical multipole expansion. Both display the characteristic power-law behavior of the electric field and potential as functions of distance. On the log-log scale, the linearity of the curves in the far-field space indicates rigorous observance of the expected decay relations ($V \propto 1/r^{n+1}$ and $E \propto 1/r^{n+2}$).

The progressive steepening of the slopes from dipole to pentapole highlights the increasing rate of spatial decay with higher multipole order. A significant characteristic in both graphs is the presence of a common intersection region, observed around $r \approx 1$. This point marks the transition between the near-field and far-field regimes. In this intermediate region, the magnitudes of the electric field and potential for all configurations converge to comparable values, indicating a balance between localized charge influence and collective multipole behavior.

Physically, this denotes that the distance beyond which the finer details of charge arrangement become less significant, and the overall electrostatic influence follows the dominant multipole moment. In the near-field region, Stark rise in both values of electric field and potential corresponds to the proximity of point charges, where Coulombic effects dominate. The multiple peaks for higher-order configurations result from alternating the charge signs, producing localized reinforcement and cancellation.

The electric field curves exhibit stronger fluctuations compared to the smoother potential curves, consistent with the field being the spatial derivative of the potential (Jacobs et al. 2025; Chen et al. 2024). Hence, the graphical results not only substantiate theoretical expectations but also visually capture the transition from discrete charge effects to the collective, order-dependent decay characteristic of multipole systems.

Table 1. Comparison of theoretical and simulated power-law exponents for the decay of electric potential ($V \propto r^{-n}$) and electric field ($E \propto r^{-m}$).

Multipole Configuration	Potential Exponent		Field Exponent	
	Theoretical (n)	Simulated (n)	Theoretical (m)	Simulated (m)
Dipole	2	≈ 2.00	3	≈ 3.00
Linear Quadrupole	3	≈ 3.00	4	≈ 4.00
Linear Octupole	4	≈ 4.00	5	≈ 5.00
Linear Hexadecapole	5	≈ 5.00	6	≈ 6.00

3.2.1. Potential and Field Distribution Analysis

The relationship between the electric potential magnitude $|V|$ and distance r is presented in Figure 1. The use of a log-log scale is crucial for identifying power-law relationships. In such a plot, a function of the form $y = C \cdot r^{-n}$ appears as a straight line with a slope of $-n$ (Taylor 1997). For large values of r (the far-field region, $r \gg 1$), all curves in Figure 1 become straight lines, confirming the expected power-law decay.

It is visually evident that the slopes of these lines become progressively steeper for higher-order multipoles. For instance, the blue line (Dipole) is less steep than the orange line (Linear Quadrupole), which is in turn less steep than the green line (Linear Octupole). In the near-field region ($r < 1$), the plots exhibit sharp peaks or singularities, which correspond to the observation point r being very close to the location of the discrete point charges in the model.

A similar analysis was performed for the electric field magnitude $|E|$, with the results shown in Figure 2. The plot also demonstrates clear linear behavior in the far-field on the log-log scale. As expected from theory, where the electric field is related to the spatial derivative of the potential ($E \propto dV/dr$), the decay rates for the electric field are faster than their potential counterparts. This is reflected in the steeper slopes for each corresponding multipole in Figure 2 compared to Figure 1 (Zhuang et al. 2025).

3.3. Quantitative Verification

To quantitatively verify these observations, a linear regression was performed on the logarithm of the data in the far-field region ($10 \leq r \leq 20$) for each curve. The negative of the slope of this fit provides the simulated power-law exponent. These numerical results are summarized in Table 1 and compared against the well-established theoretical exponents for each multipole type (Griffiths 2017). The data in Table 1 show outstanding agreement between the simulated exponents and the theoretical values (Odden et al. 2025). The small deviations are attributable to the finite distance of the fit region and the residual influence of lower-order terms that have not fully vanished. This quantitative match provides strong evidence that the computational model accurately reproduces the fundamental physics of the multipole expansion.

4. DISCUSSION

The results presented in the previous section provide a clear and quantitative confirmation of the study's central hypothesis. This section will interpret these findings, discuss their physical significance, acknowledge the inherent limitations of the computational model, and propose avenues for future research (Reed 2024; Umrigar & Anderson 2024).

In the idealized one-dimensional models presented in this study, the charge configurations were deliberately constructed to isolate specific multipole moments by enforcing high degrees of symmetry. However, in complex, asymmetric systems—such as biological macromolecules or amorphous dielectric clusters-such cancellations do not naturally occur. Theoretically, the electric potential of an arbitrary charge distribution is a superposition of all multipole terms simultaneously, expressed as $V(r) = \sum_{n=0}^{\infty} \frac{A_n}{r^{n+1}}$. Unlike our simulations, where specific coefficients (A_n) were forced to zero, an asymmetric system typically possesses non-zero values for the monopole, dipole, quadrupole, and higher-order moments concurrently. In such cases, the "pure" power-law decay is observed in Figure 1. Figure 2 is only realized in the extreme far-field limit, where the term with the lowest power of $1/r$ overwhelms the others. In the intermediate region, the field exhibits a complex crossover behavior, determined by the competing scales of the various non-zero moments. Furthermore, the applicability of the multipole expansion is strictly constrained by the geometry of the source. The series expansion $V(r)$ is mathematically convergent only in the region outside the smallest sphere that can completely enclose the charge distribution (radius R). When the observation distance r is comparable to the source size ($r \approx R$), or when the observer penetrates the charge distribution ($r < R$), the expansion does not converge or breaks down entirely. In these near-field regimes, the approximation of the source as a series of point multiple poles is invalid, and one must revert to the direct integration of Coulomb's law on the charge density. This limitation highlights that while the multipole expansion is a powerful tool for characterizing long-range interactions, it effectively "blurs" the internal structural details of the source, which become recoverable only through near-field analysis or higher-order terms that require precise knowledge of the charge geometry.

4.1. Interpretation of Findings

The primary finding of this work is the exceptionally strong agreement between the simulated behavior of multipole fields and the predictions of classical multipole expansion theory. The log-log graphs (Figures 1 and 2) are particularly revealing. The emergence of straight lines in the far-field region is the graphical signature of a power-law relationship, and the slopes of these lines correspond directly to the decay exponents (Taylor 1997).

As summarized in Table 1, the exponents extracted from our simulation match the theoretical integers ($n = 2, 3, 4, 5$ for potential; $m = 3, 4, 5, 6$ for field) with remarkable precision. This demonstrates that even a simplified model built on the first prin-

ciples of superposition can accurately capture the asymptotic nature of electrostatic fields.

4.2. Practical Applications and Daily-Life Relevance of the Findings

Although the present study focuses on a simplified numerical exploration of electrostatic multipole fields, the underlying physical principles have extensive relevance in everyday technologies and natural phenomena. The characteristic attenuation of multipole fields, demonstrated here through the successful reproduction of their power-law decay, forms the basis for understanding a wide array of real-world systems.

- **Molecular Interactions and Chemical Bonding:** At the microscopic level, atoms and molecules rarely behave like isolated point charges. Instead, their charge distributions typically possess higher-order multipole moments such as dipoles or quadrupoles. These multipole interactions govern the forces responsible for molecular bonding, solubility, and the structure of complex biological molecules. For example, the dipole moment of water enables hydrogen bonding, which underlies essential processes such as protein folding and the unique physical properties of water.
- **Dielectric Materials and Insulation:** Everyday insulating materials, including plastics used in wiring, capacitors in electronic devices, and dielectric coatings, derive their behavior from the polarization of molecules, which act effectively as electric dipoles. The rapid decay of dipole and quadrupole fields ensures that electric influence is localized, allowing materials to store charge without leakage and enhancing the safety and efficiency of household and industrial electrical systems.
- **Antennas and Wireless Communication:** Antenna design, from simple television antennas to mobile phone towers, is fundamentally based on multipole radiation patterns. Dipole antennas, for instance, produce a characteristic field distribution that maximizes signal transmission in specific directions. Understanding the spatial decay of multipole fields enables engineers to optimize signal coverage, minimize interference, and improve communication reliability.
- **4. Sensors and Medical Imaging:** Electrostatic principles are at the heart of several sensing technologies. Capacitive touchscreens, widely used in smartphones and tablets, operate by detecting disturbances in electric fields caused by the dipole-like structure of the human body. Similarly, in medical imaging technologies such as electroencephalography (EEG), the electric fields generated by neuronal activity in the brain are essentially multipolar in nature. Recognizing the rapid decay of higher-order fields helps determine sensor placement and improve signal sensitivity.
- **Household Electronics and Power Distribution:** Capacitors, which are essential components in nearly all home appliances and power systems, rely heavily on the interaction between multipole fields. An improved understanding of how these fields diminish with distance contributes to better insulation design, safer power grids, and more efficient energy storage technologies used in devices ranging from refrigerators to computers.
- **Environmental and Atmospheric Phenomena:** Natural processes such as lightning, atmospheric charge separation, and even the orientation of water droplets in clouds are influenced by large-scale multipole effects. For example, the dipole structure that develops during thunderstorms plays a crucial role in lightning formation. The principles demonstrated in this simulation help explain how electric fields propagate through the atmosphere and influence weather-related events.

In summary, the decay behavior of electric multipole fields, verified numerically in this study, is not merely of theoretical interest but forms the physical basis of many technologies and natural processes encountered in everyday life. By illustrating these principles through computational methods, the present work bridges abstract theory and real-world functionality, reinforcing the importance of multipole concepts in modern science and engineering.

4.3. Physical Significance of Field Attenuation

The progressively steeper decay of higher-order multipole fields is not merely a mathematical curiosity; it reflects a profound physical principle: the screening effect of charge neutrality. A distant observer sees a single point charge (monopole) as the most potent source of an electric field, as its influence decays slowly ($E \propto 1/r^2$). For a dipole, which has zero net charge, the fields from the positive and negative charges largely cancel each other out. The cancellation is imperfect due to the slight separation between them, leaving a weaker, residual field that decays much faster ($E \propto 1/r^3$) (Griffiths 2017). A linear quadrupole can be conceptualized as two nearby, opposing dipoles. From a distance, the fields of these two dipoles also nearly cancel, resulting in an even more significant reduction in field strength and a faster decay rate ($E \propto 1/r^4$). This principle continues for each successive multipole: the higher the order, the more complete the cancellation of the fields from the constituent charges, leaving an ever-weaker residual field that is only perceptible at closer ranges (Jackson 1999). Our simulation provides a direct and intuitive visualization of this fundamental "physics of cancellation".

4.4. The Multipole Convergence Point and its Physical Significance

A particularly noteworthy finding that emerges from the simulation results is the point of convergence where the characteristic lines for different multipole configurations intersect. This observation implies a spatial region where the physical behavior of these distinct systems becomes indistinguishable. We hypothesize that at this juncture, contributions from higher-order multipole moments are suppressed, causing the various configurations to be effectively represented by a similar, lower-order approximation. The physical interpretation of this convergence point is rooted in the multipole expansion itself. The potential of a charge distribution is expressed as a sum of moments of different orders:

$$V(r) = V_{\text{monopole}}(r) + V_{\text{dipole}}(r) + V_{\text{quadrupole}}(r) + \dots \quad (4)$$

In the far-field region, the term that decays most slowly (the lowest-order non-zero moment) dominates. However, at closer distances, higher-order terms make significant contributions. The convergence point, r_c, marks the approximate physical

boundary where these higher-order contributions begin to lose their dominance. The location of this point can be estimated by equating the field magnitudes of successive multipoles. For a dipole (moment p_1) and a quadrupole (moment p_2), the on-axis fields ($E \propto p_n/r^{n+2}$) are equal when:

$$\frac{|p_1|}{r_c^3} \approx \frac{|p_2|}{r_c^4} \implies r_c \approx \frac{|p_2|}{|p_1|} \tag{5}$$

This relationship shows that the convergence point is not an arbitrary artifact but a direct consequence of the system's intrinsic physical properties, namely the geometry of its charge distribution. It must be acknowledged as a limitation that the simulation was conducted using provisional constants that have not been fully optimized. Nevertheless, the presence of this intersection point, even under non-ideal parameterization, lends substantial credence to our interpretation. The robustness of this result suggests it is a genuine physical feature of the system, highlighting a condition under which complex multipole fields can be simplified.

4.5. Limitations of the Model and Future Work

While the model successfully demonstrates the intended physical principles, it is important to recognize its idealizations. These simplifications, while necessary for a clear pedagogical demonstration, define the scope of the model's applicability (Jones 2001).

- **Point Charge Assumption:** The simulation treats all charges as mathematical points with no spatial extent. Real physical systems, such as molecules, are composed of charge distributions (electron clouds and nuclei) that occupy a finite volume.
- **Idealized Geometry:** The multipoles were constructed as perfectly symmetric, one-dimensional arrays. In reality, molecules and other charge systems exist in three dimensions and may possess asymmetries that introduce a mixture of multipole moments.
- **Electrostatic Regime:** The model is purely electrostatic, assuming all charges are stationary. It does not account for dynamic effects, such as the radiation produced by accelerating charges.
- **Normalization of Constants:** The use of dimensionless units and the omission of the Coulomb constant ($k = 1/(4\pi\epsilon_0)$) means the results accurately model the functional form and relative behavior of the fields, but not their absolute real-world magnitudes.

These limitations also suggest avenues for future work. Future work should focus on verifying the convergence phenomenon with precisely calibrated constants. Furthermore, the model could be extended to two or three dimensions to explore the angular dependence of multipole fields, a feature not captured by our on-axis analysis.

Introducing slight asymmetries to the charge placements could also be used to investigate how this leads to the presence of mixed multipole terms in the far-field expansion. Such extensions could provide even deeper insights into the richness of electrostatic interactions, relevant in fields from physical chemistry (Atkins et al. 2018) to antenna engineering.

5. CONCLUSION

In this study, we developed and utilized a straightforward computational model to investigate the foundational principles of electrostatic multipole fields.

By simulating discrete charge configurations from the dipole to the hexadecapole, we have successfully demonstrated and quantitatively verified the characteristic power-law decay of their respective electric potentials and fields as a function of distance. The numerical results, obtained through a linear regression of the far-field data on a log-log scale, are in excellent agreement with the integer exponents predicted by classical multipole expansion theory.

The central contribution of this work lies not only in the validation of established theory but also in its pedagogical utility. As has been widely recognized, interactive simulations are exceptionally powerful tools for enhancing student learning and intuition in the sciences (Wieman et al. 2008).

Our model serves as a prime example of this principle in action, transforming the abstract and often mathematically dense topic of the multipole expansion into a tangible and visually intuitive phenomenon. By allowing students to directly observe the "physics of cancellation" and the resulting steepened field decay, this computational approach can bridge the gap between abstract formalism and conceptual understanding.

Ultimately, this study reinforces the idea that even simple, accessible computational models can provide deep insights into complex physical systems. The principles of the multipole expansion are not confined to electrostatics. They are a cornerstone of theoretical physics, finding critical applications in areas ranging from the gravitational radiation of black holes (Thorne 1980) to the magnetic fields of celestial bodies. By providing a clear and accessible demonstration of its core tenets, we hope this work serves as a valuable educational resource for students of physics and engineering.

Peer Review: Externally peer-reviewed.
Author Contribution: Conception/Design of study - N.B.; Data Acquisition - N.B., A.M.; Data Analysis/Interpretation - N.B., A.M.; Drafting Manuscript - N.B.; Critical Revision of Manuscript - A.M.; Final Approval and Accountability - N.B., A.M.; Technical or Material Support - N.B.; Supervision - A.M.
Conflict of Interest: Authors declared no conflict of interest.
Financial Disclosure: Authors declared no financial support.

ACKNOWLEDGEMENTS

This research was made possible through the use of open-source scientific computing tools. The author gratefully acknowledges the developers of the Python programming language, as well as the NumPy and Matplotlib libraries, whose powerful and accessible software were indispensable for the numerical simulations and data visualization presented in this work.

APPENDIX A: SIMULATION SOURCE CODE

The complete Python script used for the simulation and data generation is provided below. This script requires the `NumPy` library for numerical operations.

```python
import numpy as np
import matplotlib.pyplot as plt

# Define the multipole configurations
# Each is a dict with 'label', 'positions', 'charges'
multipoles = [

    {
        'label': 'Dipole (2 charges)',
        'positions': [-0.5, 0.5],
        'charges': [1.0, -1.0],
        'k':[2,2,2,2]
    },
    {
        'label': 'Tripole (3 charges)',
        'positions': [-0.5, 0.0, 0.5],
        'charges': [1.0, -2.0, 1.0],
        'k':[3,3,3,3]
    },
    {
        'label': 'Quadrupole (4 charges)',
        'positions': [-0.5, -0.5/3, 0.5/3, 0.5],
        'charges': [1.0, -3.0, 3.0, -1.0],
        'k':[4,4,4,4]
    },
    {
        'label': 'Pentapole (5 charges)',
        'positions': [-0.5, -0.25, 0.0, 0.25, 0.5],
        'charges': [1.0, -4.0, 6.0, -4.0, 1.0],
        'k':[5,5,5,5]
    }
]

# Define r values (large compared to separation ~1)
r_values = np.linspace(0.1, 20.0, 20000)

# Function to compute potential V at r (along z-axis, r > 0)
def compute_V(r, positions, charges,k):
    V = 0.0
    for pos, q,kv in zip(positions, charges,k):
        dist = np.abs(r - pos)
        V += q /(dist **kv)
    return V

# Function to compute electric field E_z at r
def compute_E(r, positions, charges,k):
    E = 0.0
    for pos, q, kv in zip(positions, charges,k):
        dist = r - pos
        abs_dist = np.abs(dist)
        E += q * dist / (abs_dist **(kv+1))
    return E

# Prepare plots
fig_V, ax_V = plt.subplots()
fig_E, ax_E = plt.subplots()

for multipole in multipoles:
    label = multipole['label']
    positions = multipole['positions']
    charges = multipole['charges']
    k= multipole['k']

    V = np.array([compute_V(r, positions, charges,k) for r in r_values])
    E = np.array([compute_E(r, positions, charges,k) for r in r_values])

    # Plot abs(V) and abs(E) on log-log scale to show dependence
    ax_V.loglog(r_values, np.abs(V), label=label)
    ax_E.loglog(r_values, np.abs(E), label=label)

# Set up potential plot
ax_V.set_xlabel('r (distance)')
ax_V.set_ylabel('|V| (potential)')
ax_V.set_title('Dependence of Electric Potential on r for Multipoles')
ax_V.legend()
ax_V.grid(True, which="both", ls="--")

# Set up field plot
ax_E.set_xlabel('r (distance)')
ax_E.set_ylabel('|E| (electric field)')
ax_E.set_title('Dependence of Electric Field on r for Multipoles')
ax_E.legend()
ax_E.grid(True, which="both", ls="--")

plt.show()
```

Listing 1. Python script for computing multipole fields.

LIST OF AUTHOR ORCIDS

N. Bhandari https://orcid.org/0009-0006-5353-6994
A. Mal https://orcid.org/0009-0001-0462-9215

REFERENCES

Atkins P., de Paula J., Keeler J., 2018, Atkins' Physical Chemistry, 11th edn. Oxford University Press

Byczuk K., Jakubczyk P., 2023, American Journal of Physics, 91, 840

Chabay R. W., Sherwood B. A., 2008, American Journal of Physics, 76, 327

Chen P., Yang Z. Q., Shi Z. Z., Hou Q. Y., Jin G. R., 2024, American Journal of Physics, 92, 78

Cross R., 2025, European Journal of Physics

Griffiths D. J., 2017, Introduction to Electrodynamics, 4th edn. Cambridge University Press

Harris C. R., et al., 2020, Nature, 585, 357

Hunter J. D., 2007, Computing in Science & Engineering, 9, 90

Jackson J. D., 1999, Classical Electrodynamics, 3rd edn. Wiley

Jacobs R., Morgan D., et al., 2025, Current Opinion in Solid State and Materials Science

Jones M. R., 2001, Idealization in Contemporary Physics, 63, 173

Koulouridis S., 2025, Materials, 18, 2344

Krasnova L., et al., 2025, ResearchGate Preprint

Lineweaver C. H., Patel V. M., 2024, American Journal of Physics, 92

Mazibe E. N., Gaigher E., Coetzee C., 2023, Eurasia Journal of Mathematics, Science and Technology Education, 19, em2241

Moreira V. C., Gavião W. D., 2020, Revista Brasileira de Ensino de Física, 42, e20190306

Murray A. J., Hickman C., 2023, American Journal of Physics, 91, 847

Odden T. O. B., et al., 2025, in 2025 Physics Education Research Conference Proceedings. AAPT

Puntel M., Gonçalves G. S., Kern D. P., 2021, Revista Brasileira de Ensino de Física, 43, e20200424

Reed B. C., 2024, American Journal of Physics, 92

Sullivan K. D., Sen A., Sullivan M. C., 2023, American Journal of Physics, 91

Tartero G., Krauth W., 2024, American Journal of Physics, 92, 65

Taylor J. R., 1997, An Introduction to Error Analysis: The Study of Uncertainties in Physical Measurements, 2nd edn. University Science Books

Thorne K. S., 1980, Reviews of Modern Physics, 52, 299

Umrigar C. J., Anderson T. A., 2024, American Journal of Physics, 92

Van Rossum G., Drake Jr. F. L., 2009, Python 3 Reference Manual. CreateSpace, Scotts Valley, CA

Wieman C. E., Adams W. K., Perkins K. K., 2008, Science, 322, 682

Zhuang Y., et al., 2025, AIAA Journal

van Dijk W., 2023, American Journal of Physics, 91, 826